Mountain Pine Beetle Red-Attack Forest Damage Classification Using Stratified Landsat TM Data in British Columbia, Canada

S.E. Franklin, M.A. Wulder, R.S. Skakun, and A.L. Carroll

Abstract

The identification and classification of mountain pine beetle, Dendroctonus ponderosae *(Hopkins), red-attack damage patterns in a mature lodgepole pine (*Pinus contorta*) forest located in the Fort St. James Forest District, British Columbia, was accomplished using 1999 Landsat TM satellite imagery, 1999 mountain pine beetle field and aerial survey point data, and GIS forest inventory data. Unrelated variance in the observed spectral response at mountain pine beetle field and aerial survey points was reduced following image stratification with the GIS forest inventory data and removal of other factors uncharacteristic of red-attack damage. Locations of known mountain pine beetle infestation were used to train a maximum-likelihood algorithm; overall classification accuracy was 73 percent, based on an assessment of 360 independent validation points. If local stand variability is reduced prior to signature generation, accuracies and map products can be useful for those involved in active forest management decision-making regarding mountain pine beetle infestations.*

Introduction

Infestations of mountain pine beetle, *Dendroctonus ponderosae* (Hopkins), are a major forest disturbance affecting mature lodgepole pine (*Pinus contorta*) stands in western North America. In many areas of the central interior region of British Columbia, populations of mountain pine beetle have reached epidemic proportions, possibly as a result of successive years of favorable weather conditions and abundant reserves of mature pines. Outbreaks commonly spread over the landscape causing widespread damage, usually expressed as the mortality of hundreds of thousands of lodgepole pine trees, and are typically not confined to individual forest stands. This resultant mortality of trees compromises efforts towards sustainable forest management. Lodgepole pine also accounts for more than half of the growing stock in the central interior and is the dominant species of commercially harvested timber in the province.

There are four distinct stages in a mountain pine beetle infestation cycle: endemic, incipient, outbreak, and collapse. Endemic infestations—small populations of widely dispersed beetles—usually grow into an incipient stage and then progress into an outbreak stage when groups of infested trees coalesce into larger patches. Outbreaks collapse when the supply of suitable pines is exhausted. Effective management of the mountain pine beetle is dependent upon rapid and accurate detection of population stage and trend (i.e., increasing or decreasing). Control or suppression is only feasible for endemic or incipient populations (e.g., Carroll and Linton, 2002). Most beetle detection programs involve a traditional approach based on aerial surveys. In this approach, an observer views the forest canopy in a fixed-wing aircraft and looks for signs of attacked trees, that is, dying trees whose foliage is turning from green to red. The boundaries of foliage reddening are then mentally averaged and delineated onto a sketch map. Ground surveyors are often used to verify the cause of the disturbance and assess the severity of forest damage. The drawbacks of using these surveying methods are the high operation costs and many hours of manpower required. Also, mountain pine beetles often spread and colonize new areas before an infested area has been completely surveyed by ground or air.

Mountain pine beetle attacks may first create a pre-visual signal, known as the green-attack stage, which may become detectable within foliage during the fall and early winter, or approximately 2 to 3 months after initial attacks. This stage results from changes to the cellular structures of the foliage (Murtha, 1978; Murtha and Wiart, 1987), likely due to water deficiency as a result of interrupted translocation caused by the mining of beetle larvae in the phloem and the colonization of the sapwood by pathogenic bluestain fungi introduced to the tree on attack (Safranyik *et al.*, 1974). Visually, damage is often first apparent during the spring of the following year of an attack as foliage becomes yellow (i.e., chlorotic) then bright red (Plate 1). Foliage discoloration in this stage is caused by chlorophyll degradation as the foliage dies (Murtha, 1978). In one study, current red-attack foliage was brighter than foliage on non-attacked trees in the 520- to 640-nm range (Ahern, 1988). This higher reflectance was thought to be caused by a reduced amount of chlorophyll in the attacked foliage or by a shorter optical path because of decreased scattering by a less-developed cell structure. The grey-attack stage occurs approximately 2 to 3 years after initial attack as the dead needles are shed, leaving the grey-colored stems and branches (Unger, 1993).

S.E. Franklin and R.S. Skakun are with the Department of Geography, University of Calgary, Calgary, Alberta T2N 1N4, Canada (franklin@ucalgary.ca).

M.A. Wulder and A.L. Carroll are with the Canadian Forest Service, Pacific Forestry Centre, Victoria, British Columbia V8Z 1M5, Canada.

Photogrammetric Engineering & Remote Sensing
Vol. 69, No. 3, March 2003, pp. 283–288.

0099-1112/03/6903–283$3.00/0

Research to detect and classify red-attack damage and forests severely infested by mountain pine beetles using remotely sensed data, acquired from sensors such as the Landsat Thematic Mapper (TM) (Renz and Nemeth, 1985) and by aerial multispectral sensors (Gimbarzevsky *et al.*, 1992), has been well documented, but few operational examples exist. The main problems have been twofold: (1) there is a very high degree of natural variability in forests affected by the beetle, and (2) there is a relatively small influence of beetle damage on spectral response, particularly as measured by broadband satellite sensors, unless very large and homogeneous areas are affected. In one study, Sirois and Ahern (1988) interpreted SPOT HRV color composites and concluded that the minimum red-attack damaged area was 1 to 2 ha in size wherein more than 80 percent of the crowns were red. This threshold of detection was too great to be practical for mountain pine beetle control programs which typically require the detection of five or more trees within an area much less than one hectare. One way of reducing large natural variability, and simultaneously isolating the spectral distinctiveness of the beetle-induced changes to forest canopies, is to employ stratification techniques. Franklin and Raske (1994) used forest structure strata obtained from a GIS forest inventory database to increase SPOT and Landsat TM classification of "red-stage" spruce budworm (*Choristoneura fumiferana* Clem.) defoliation by up to 30 percent. When considering satellite remote sensing in the detection and classification of mountain pine beetle damage, the development of strata likely requires a judicious use of the available imagery together with field, aerial survey, and GIS data.

In this study, red-attack damage caused by mountain pine beetle infestation was classified using Landsat TM imagery, acquired on 12 September 1999, within strata developed from GIS forest inventory data and with reference to field data and aerial survey information. The field and aerial survey dataset was collected in the Prince George Forest Region from 09 August to 10 September 1999. Trained field and aerial observers mapped three red-attack damage classes: less than 10, 10 to 20, and 21 to 50 red-attacked trees in approximately 50-meter-diameter plots across a large mountain pine beetle forest infestation. These observations were later combined into a single red-attack damage class which could then be compared to samples obtained in non-attacked forest stands of similar composition and structure. A maximum-likelihood classifier based on training areas developed from the field and aerial samples was used to classify the satellite image to determine the occurrence of red-attack beetle damage. Accuracy was assessed using an independent sample of known damage sites. The result of the red-attack damage classification was a map showing stands with a high likelihood of containing small groups of red-attack trees.

Figure 1. Location of the study area in central British Columbia.

Study Area and Data Collection

The 5070 km^2 study area is located in the lower southern half of the Fort St. James Forest District and extends into the northeast and northwest corners of the Vanderhoof and Prince George Forest Districts in British Columbia (Figure 1). There are no areas of significant relief on either a large or small scale. The main forest species in the study area include lodgepole pine, white spruce (*Picea glauca*), Engelmann spruce (*Picea engelmannii*), black spruce (*Picea mariana*), trembling aspen (*Populus tremuloides*), and Douglas fir (*Pseudotsuga menziesii*), with a smaller component of western red cedar (*Thuja plicata*) and sub-alpine fir (*Abies lasiocarpa*) (Table 1). Based on these forest species, lodgepole pine stands were one of the youngest (104 years) and most dense in terms of canopy closure (51 percent). The lodgepole pine stands also cover approximately 61 percent of the total forested area. Aspen and Douglas fir stands occur more frequently along the western margins of the study area. Higher elevations in the northern interior contain most of the sub-alpine fir. Forest harvesting operations are most active along the eastern half and northern interior. Many of the cut-blocks are less than 15 years of age; lodgepole pine and white spruce are the main forest species planted or regenerated naturally.

The mountain pine beetle field and aerial survey point dataset was collected from 09 August to 10 September 1999. An observer in a helicopter counted the number of red-attack trees directly below the aircraft, at a flying altitude of 30 to 60 meters, and recorded the location of each infestation and number of red-attack trees into one of three categories: less than 10, 10 to 20,

TABLE 1. TYPE OF FOREST SPECIES AND THEIR ASSOCIATED STRUCTURAL COMPONENTS IN THE STUDY AREA

Species	Code	Area (ha)	Volume (m^3)	[1]DBH (cm)	[2]CC (%)	Age (years)	Height (m)
W. Red Cedar	AC	60.0	8,321.0	31.3	33	109	25.7
Trembling Aspen	AT	3,773.3	246,998.6	21.6	45	86	19.8
Sub-alpine Fir	ALF	804.0	59,691.1	23.8	44	127	37.6
Douglas Fir	FD	940.5	113,040.3	30.1	47	137	25.4
Lodgepole Pine	PL	23,274.8	2,649,161.6	22.7	51	104	21.8
Engelmann Spruce	ES	1,863.4	199,962.5	19.4	34	105	18.1
Black Spruce	SB	1,520.8	630,788.1	9.4	33	124	11.2
White Spruce	SW	6,034.5	1,024,565.4	27.7	41	128	24.9
Total		38,271.3					

[1]DBH = diameter breast height, [2]CC = canopy closure

and 21 to 50 trees (M. Paulson, TerraPro GPS Surveys Ltd., personal communication). For example, a point collected in the less-than-ten-tree category represents an epicenter containing less than ten red-attack trees in an approximate 50-meter-diameter plot area. A ground crew then walked an area around a sample of these sites and recorded the following field data:

- type of attacking bark beetle(s) specie(s) (up to four);
- possible fire and water damage at the site;
- location near road, cut-block edge, swamp, creek, lake, or beside salvage and poor site conditions;
- presence of faders (synonymous with red-attack trees); and
- single and scattered red-attack and grey-attack (number of trees).

The location of each field and aerial survey site was recorded in real GPS time and projected to a UTM NAD83 Zone 10 projection. In total, 2249 mountain pine beetle field and aerial survey points were recorded in the study area. The majority of these were located along the western half of the study area, where harvesting of lodgepole pine was most active. Most of the observations were in the less-than-ten-tree category, which comprises 82 percent of the total mountain pine beetle field and aerial survey points.

A GIS forest inventory polygon dataset was used to develop strata of the forest composition and structure in the study area. Each of the forest polygons contained a large number of attribute data, including species composition, stand age (years), canopy closure (to the nearest 10 percent), height (m), dbh (diameter breast height, cm), volume (m^3), and area (ha). The dataset was structured in vector format (1:250,000 scale) and projected to UTM Zone 10 on the NAD83 datum to facilitate geometric correction and overlay of the image and mountain pine beetle survey data. The data for the forest stands were projected (or date-stamped) for 01 January 1999.

The satellite data consisted of a Landsat TM image (Path/Row: 49/22) acquired on 12 September 1999, with approximately 0 percent cloud cover. The image solar conditions were 38.6° sun elevation and 160.3° sun azimuth. The image was first geometrically corrected to the GIS forest inventory dataset, using a cubic-convolution resampling algorithm and 40 ground control points at key road intersections dispersed throughout the scene, and then atmospherically corrected based on a standard atmospheric model as described by Richter (1990). In this atmospheric correction program, the ground visibility is first determined for the image scene. Then the program used this estimate of the ground visibility, along with the type of atmosphere and the aerosol type, the average elevation constant, calibration coefficients, image acquisition data, and the solar zenith angle, to calculate the reflectance from the image DN values. The mountain pine beetle field and aerial survey data points were then overlayed on the TM image (Plate 2).

Analytical Methods

A supervised classification approach was adopted based on the large number of possible training area pixels contained in the field and aerial survey dataset. This dataset was stratified such that a red-attack signature was obtained from pixels with a high degree of confidence that these pixels represented red-attack damage at the time of image acquisition. A similar sample was developed from healthy stands in the area to train a non-attacked forest class. First, a forest structure mask was generated based on a set of host susceptibility factors. Safranyik *et al.* (1974) suggested that stand susceptibility to mountain pine beetle increases "with trees over 60 years of age and stands with a high pine component." We removed from further consideration all field sample points which were located in polygons composed of less than 40 percent lodgepole pine or which were less than 60 years of age. Of the polygons remaining, 93 percent were composed of lodgepole pine as the dominant species covering an area approximately 19,100 ha. Involving a data stratification procedure proved to be an important component in reducing unrelated variance in the spectral response and creating the desired red-attack spectral response patterns to generate a spectral signature.

Some spruce beetle (*Dendroctonus rufipennis*) and western balsam bark beetle (*Dryocoetes confusus*) infestation occurred and, where noted in the field sample, were deleted. A similar screening decision-rule was applied to remove grey-attack points from the sample to avoid possible confusion with red-attack spectral response during classification. Finally, an edge filter was used to delete points located near and on the edges of cut-blocks, roads, rivers, and lakes in order to reduce spectral variability caused by edge effects.

The resulting mountain pine beetle red-attack training area comprised 360 sites from only those areas observed in the field or the aerial survey which were likely to have suffered mountain pine beetle red-attack damage at the time of the data collection. We acquired a similar size training area for non-attacked forest by sampling from the large number of polygons in the GIS which did not contain beetle damage but which satisfied the stratification criteria. Overall, more than 700 pixels were used in the generation of these two signatures, which were then tested for suitability as input to the maximum-likelihood algorithm based on the full set of TM bands. The spectral response values in each TM band of the red-attack training area pixels were very close to a normal distribution (Table 2). Singularity and multicollinearity were assessed to determine the redundancy of the variables. Singularity represents a perfect correlation ($r = 1$) between variables, which did not exist in the correlations between the TM bands. Also, there were no TM band correlations greater than $|0.80|$, suggesting that the TM bands were relatively free from multicollinearity conditions (Clark and Hosking, 1986).

TABLE 2. SUMMARY STATISTICS OF THE MOUNTAIN PINE BEETLE FIELD AND AERIAL SURVEY POINTS FOR TRAINING THE LANDSAT TM CLASSIFICATION

	Univariate Statistics					
	Band 1	Band 2	Band 3	Band 4	Band 5	Band 7
Min.	24	18	13	53	21	10
Max.	36	29	26	84	60	29
Mean	30	23	18*	66*	35	17
Median	30	23	18	65	36	18
Std. Dev.	2.00	1.97	2.12	7.50	5.81	3.05
Skewness	−0.126	0.052	0.509	0.370	0.535	0.422
Kurtosis	−0.310	0.391	0.462	−0.665	1.115	0.779
	Covariance Matrix					
	Band 1	Band 2	Band 3	Band 4	Band 5	Band 7
Band 1	4.21					
Band 2	0.47	3.07				
Band 3	0.84	0.93	4.96			
Band 4	1.15	3.40	1.88	56.25		
Band 5	1.78	3.62	3.67	13.54	33.76	
Band 7	0.66	1.85	2.29	4.65	8.98	9.30
	Correlation Matrix					
	Band 1	Band 2	Band 3	Band 4	Band 5	Band 7
Band 2	0.19					
Band 3	0.22	0.36				
Band 4	0.17	0.52	0.26			
Band 5	0.21	0.55	0.40	0.65		
Band 7	0.14	0.45	0.40	0.44	0.78	

*Significant difference between non-attack class and red-attack class at 95% probability.
**All correlations significant at 90%.

Plate 1. Mountain pine beetle red-attack damage (photographed by Rob Skakun, Fort St. James area, 04 September 2001).

TABLE 3. SUPERVISED MAXIMUM-LIKELIHOOD CLASSIFICATION ACCURACY FOR THE RED-ATTACK CLASS AND NON-ATTACK CLASS

	Percent of Pixels Classified into a Class*		
	1	2	Total
From Class*			
1	71.1	28.9	100
2	26.7	73.3	100

Overall accuracy for the classification: 72.3%
Kappa classification accuracy: 35%
*Class 1 = non-attack
*Class 2 = red-attack

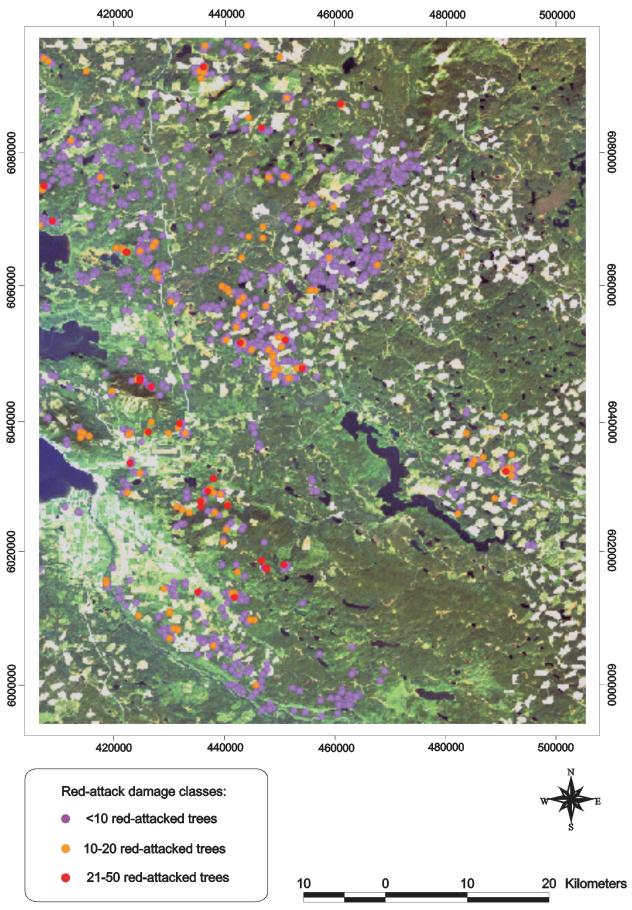

Plate 2. Project study area showing locations of field and aerial survey points overlayed on the Landsat TM image.

The maximum-likelihood algorithm is a spatially explicit classification procedure that assigns every pixel to the class to which it has the highest probability of being a class member (Jensen, 1996). We divided the training pixels into two equal samples, and reserved one of these to test the accuracy, using the other to generate class signatures for input to the maximum-likelihood procedure. Classification accuracy was assessed using a standard confusion matrix (Congalton and Green, 1999). The producer's accuracy, user's accuracy, overall accuracy, and the Kappa coefficient were generated. Overall class accuracies are interpreted here, together with a map showing red-attack damage pixels within forest stand polygons.

Results

The classification accuracy assessment revealed that overall classification accuracy was 72.3 percent (Table 3). The red-attack class was 73.3 percent correct based on the spectral response data obtained following stratification of the mountain pine beetle field and aerial survey calibration points. The non-attack accuracy of 71.1 percent is reasonable. This level of accuracy is consistent with forest classification results reported in a wide range of relatively homogeneous conifer stands and simple maximum-likelihood decision rules (e.g., Franklin and Luther, 1995). Higher classification accuracy may have been achieved with greater effort in the field to collect training areas for the non-attack forest class. The red-attack class accuracy is higher than the accuracies of mountain pine beetle red-attack damage reported previously. For example, in a study using simulated Thematic Mapper data (Renz and Nemeth, 1985), infestations greater than 1.5 ha were approximately 70 percent correct; however, for an infestation less than 1.5 ha, the accuracy was less than 40 percent. In the current study, each mountain pine beetle field and aerial point represents a single TM pixel, which, in turn, represents an ocularly-estimated (from helicopter) 50-meter-diameter plot size (much less than 1 ha).

The map of red-attacked forest stands is shown in Plate 3. Two small inset windows indicate the patchy nature of the red-attack damage class within stand polygons. Each TM pixel in the red-attack class represents at least nine red-attack trees. Polygons with several small patches represent stands in which beetles were relatively abundant (Inset A). Some relatively large homogeneous patches indicate high infestation areas (Inset B). The general appearance of the map and degree of detection is, however, consistent with the way in which mountain pine beetle infestations occurred in this area (see Sharma and Murtha, 2001). The map appears useful in decision making for forest managers for several reasons. Although it indicates only the extent of damage from the previous year's population (i.e., red-attack is the result of infestation of trees during the preceding summer), the map provides a rapid and accurate quantification of the distribution of mountain pine beetle over the landscape. This information can be used to prioritize areas for more detailed surveys of current (i.e., green) attack trees to identify stands in which to apply direct control methods, and to plan salvage logging activities. Moreover, comparison of red-attack maps among years can be used to assess population and damage trends within forest management units, and

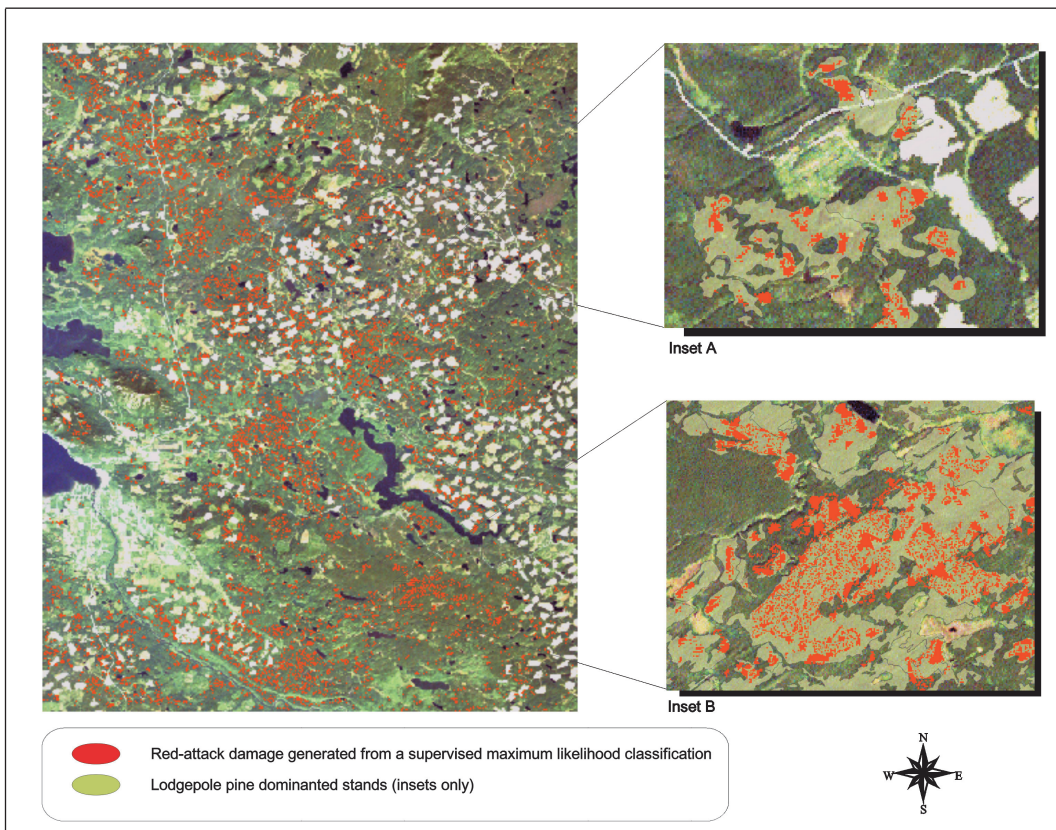

Plate 3. Classification of the mountain pine beetle red-attack damage class in the Fort St. James area.

thereby allow control efforts to focus on areas where populations are increasing.

Stratification of a large number of field and aerial survey points resulted in a distinct spectral signature for red-attack damage in relatively homogeneous lodgepole pine stands. This technique has been used to improve classification results of spruce budworm defoliation in conifer stands (Franklin and Raske, 1994). For example, 75 percent overall classification accuracy was achieved based on the classification of spruce budworm (*Choristoneura occidentalis* Free.) defoliation using Landsat TM data in western Oregon (Franklin *et al.*, 1995). In that study, stratification was accomplished using a Landsat image acquired prior to the insect infestation occurrence (see also Collins and Woodcock (1996)). However, several other methods may be considered to improve the classification accuracy still further. Multispectral data from Ikonos (1- to 4-meter spatial resolution) satellite imagery could be used for detection of small, scattered infestations, as was the case in the present study area. A sub-pixel TM analysis (Murtha, 2000) could also be performed. The sub-pixel analysis process requires individual spectral signatures of background material, and then identifies the residual spectrum that most closely matches the spectrum of the material of interest (the damage class signature). Each pixel is assigned a fraction value of the amount of endmember it contains. This is similar to fuzzy classification logic (Wang, 1990), where pixels are assigned a membership grade of the various constituent classes found in a mixed pixel.

Conclusion

Red-attack damage attributable to the mountain pine beetle in the Fort St. James Forest District was classified with Landsat TM imagery using training areas developed from a mountain pine beetle field and aerial survey point dataset. To reduce training area variability, the training areas were stratified prior to signature generation with GIS data and logical decision rules based on host susceptibility information and forest structure. This was important because the high variance in spectral response within training areas can cause an overestimation of the red-attack damage class during supervised classification procedures (Gimbarzevsky *et al.*, 1992). The maximum-likelihood classification accuracy was determined to be approximately 73 percent, based on 360 independent mountain pine beetle field and aerial survey validation points. Overall, the classification accuracy achieved in this project was higher than that obtained in earlier research with Landsat TM data and forest damage classes because spectral differences between non-attacked and red-attacked areas were enhanced through stratification. Damage caused by the mountain pine beetle was not confounded by uncontrolled natural stand variability and the relatively small spectral influence of a few damaged crowns within a small area. The final classification map showed small pockets of infestation - individual pixels within forest stands - which were likely the locations of mountain pine beetle red-attack damage.

Acknowledgments

This work was funded by a research grant from the Natural Sciences and Engineering Research Council and a research contract from the Canadian Forest Service.

References

Ahern, F.J., 1988. The effects of bark beetle stress on the foliar spectral reflectance of lodgepole pine, *International Journal of Remote Sensing*, 9:1451–1468.

Carroll, A.L., and D. Linton, 2002. Managing mountain pine beetle populations in British Columbia, *Forest Health and Biodiversity News*, 6:2–5.

Clark, W., and P. Hosking, 1986. *Statistical Methods for Geographers*, John Wiley and Sons, New York, N.Y., 518 p.

Collins, J.B., and C.E. Woodcock, 1996. An assessment of several linear change detection techniques for mapping forest mortality using multitemporal Landsat TM data, *Remote Sensing of Environment*, 56:66–77.

Congalton, R.G., and K. Green, 1999. *Assessing the Accuracy of Remotely Sensed Data: Principles and Practice*, CRC Press, Boca Raton, Florida, 137 p.

Franklin, S.E., and J.E. Luther, 1995. Satellite remote sensing of balsam fir forest structure, growth, and cumulative defoliation, *Canadian Journal of Remote Sensing*, 21:400–411.

Franklin, S.E., and A. Raske, 1994. Satellite remote sensing of spruce budworm defoliation in western Newfoundland, *Canadian Journal of Remote Sensing*, 20:37–48.

Franklin, S.E., R.H. Waring, R.W. McCreight, W.B. Cohen, and M. Fiorella, 1995. Aerial and satellite sensor detection and classification of western spruce budworm defoliation in a subalpine forest, *Canadian Journal of Remote Sensing*, 21:299–308.

Gimbarzevsky P., A.F. Dawson, and G.A. Van Sickle, 1992. *Assessment of Aerial Photographs and Multi-Spectral Scanner Imagery for Measuring Mountain Pine Beetle Damage*, Info. Rep. BC-X-333, Pacific and Yukon Region, Forestry Canadian, 31 p.

Jensen, J.R., 1996. *Introductory Digital Image Processing: A Remote Sensing Perspective*, Prentice Hall, Englewood Cliffs, New Jersey, 316 p.

Murtha, P.A., 1978. Remote sensing and vegetation damage: A theory for detection and Assessment, *Photogrammetric Engineering & Remote Sensing*, 44:1147–1158.

———, 2000. Spectral unmixing of mountain pine beetle attack, UBC Faculty of Forestry, *Branch Lines*, 11(3):4.

Murtha, P.A., and R. Wiart, 1987. PC-based digital image analysis of mountain pine beetle green attack: preliminary results, *Canadian Journal of Remote Sensing*, 13:92–95.

Renz, A.N., and J. Nemeth, 1985. Detection of mountain pine beetle infestation using Landsat MSS and simulated Thematic Mapper data, *Canadian Journal of Remote Sensing*, 11:50–57.

Richter, R., 1990. A fast atmospheric correction algorithm applied to Landsat TM Images, *International Journal of Remote Sensing*, 11:159–166.

Safranyik, L., D.M. Shrimpton, and H.S. Whitney, 1974. *Management of Lodgepole Pine to Reduce Losses from the Mountain Pine Beetle*, Forestry Technical Report No. 1, Pacific Forest Research Centre, Canadian Forestry Service, Environment Canada, Victoria, British Columbia, Canada, 31 p.

Sharma, R., and P.A. Murtha, 2001. Application of Landsat TM Tasseled Cap Transformations in detection of mountain pine beetle infestations, *Proceedings 23rd Canadian Symposium on Remote Sensing (CASI)*, 01 August, Ottawa, Ontario, Canada, 9 p. (CD-ROM).

Sirois, J., and F.J. Ahern, 1988. An investigation of SPOT HRV data for detecting mountain pine beetle mortality, *Canadian Journal of Remote Sensing*, 14:104–108.

Unger, L., 1993. *Mountain Pine Beetle*, Forest Pest Leaflet No. 76, Forest Insect and Disease Survey, Forestry Canada, 7 p.

Wang, F., 1990. Improving remote sensing image analysis through fuzzy information representation, *Photogrammetric Engineering & Remote Sensing*, 56:1163–1169.

(Received 07 January 2002; accepted 18 April 2002; revised 12 June 2002)